VI CONGRESSO NACIONAL DE ENGENHARIA MECÂNICA
VI NATIONAL CONGRESS OF MECHANICAL ENGINEERING
18 a 21 de agosto de 2010 – Campina Grande – Paraíba - Brasil
August 18 – 21, 2010 – Campina Grande – Paraíba – Brazil

On Turbulent Flow in Closed compound Channels

J.N.V.Goulart, jvaz@unb.br[1]
S. V. Möller, svmoller@.ufrgs.br[2]

[1]Faculdade UnB Gama – Universidade de Brasilia
Área Especial 2, Lote 14
Setor Central – Gama, DF, Brasil
Cep: 72405-610

[2]PROMEC – Universidade Federal do Rio Grande do Sul
Rua Sarmento Leite, 425
Porto Alegre – Rio Grande do Sul, Brasil
cep: 90050 – 170

Abstract: *Hot wire annemometry tchenique was employed to know main features of developing turbulent flow in two kinds of closed compound channel. The first one consist in two rectangular tubes attached on a side wall of a wind channel apart from one each other by a distance "d", forming a narrow gap. Second compound channel is formed by the same tubes, but this time attached on the top and bottom walls of the wind channel, building two main channels connected by a narrow gap with width "d". Results showed this sort of geometry gives rise an intersting flow, quite similar to the spatial developing mixing layer. Velocity profiles were also investigated. All of them presented high vorticity peaks at the main channel/subchannel interface, indicating large scales structures may be present in the flow. By using quantities from mean flow a Strouhal number was purposed. Regardless the kind of channel, the dimensionless frequency was almost constant for Strouhal number 0.10.*

Palavras-chave: *turbulence in compound channels, hot wire annemometry, mixing layer, large scale structures*

1. INTRODUCTION

Compound channels are characterized by the presence of a narrow region connecting one or more main channels, Figure 1. The narrow gaps are responsible for mass, energy and momentum exchanging between main subchannels.

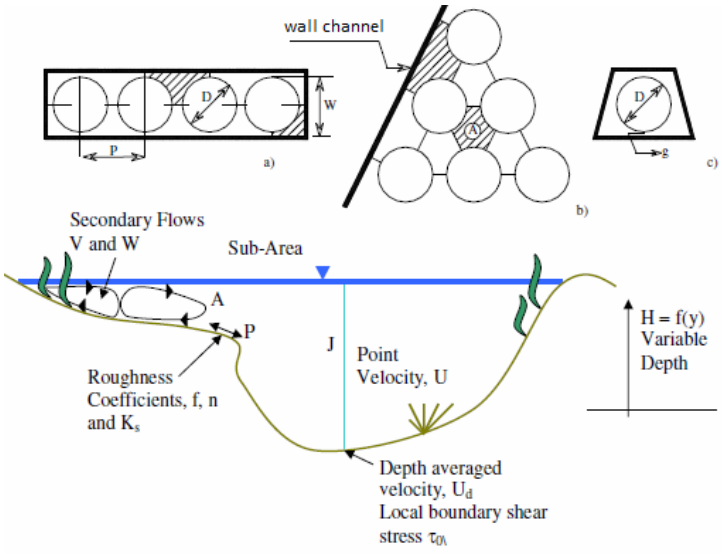

Figure 1 – Examples of compound channels

These geometries are present in many areas of the engineering, as nuclear reactors, steam generators and some kinds of water channels. On the mechanical engineering field the problems are often linked to heat exchangers, nuclear reactor fuel elements and even electronic devices. On the last ones, the main goal is rising heat exchange rates.

As remarkable features of these kinds of channels are the unusual Reynolds stresses distribution and the sinusoidal patterns of the velocities series taken from these channels, as well. Being these facts very well reported by Knight and Shiono (1990), Soldini et al., (2004), when the authors studied open compound channels. Related to closed compound channels the works from Meyer and Rehme (1994 and 1995), showed similar results those previously found in open channels.

Despite unusual Reynolds stress distribution, the main source of interest has lain on the unexpected sinusoidal patterns of velocity fluctuations near the gap. The quasi-periodical behavior of the velocity fluctuations was named flow pulsations.

Flow pulsations occurrence was reported, at the first time, by Rowe (1973), when the author studied mixture process of the turbulent flow in a rod bundle. According to author, the frequency associated to this phenomenon increased when the gap width was reduced. By using hot wires probes Möller (1991), confirmed Rowe's findings, therefore, his results also showed flow pulsations were associated to strong field of vorticity near the gap.

Quasi-periodical flow pulsations were also found in other kind of compound channel, showing this phenomenon was not restricted to rod bundles assembly. Wu and Trupp (1994), performed hot wire measurements in a trapezoidal channel containing a single tube. The results showed pronounced peaks in spectra, confirming the strong dependence of the frequency on geometrical parameters and the flow velocity. After that, Meyer and Rehme (1994) and Meyer and Rehme (1995), performed measurements in unusual compound channels. By using hot wire anemometry, the authors studied the flow characteristics in a channel with two or several parallel fins attached to a side wall. The geometry was quite similar to an internally finned channel, forming slots connected to main channels. Test sections were characterized by dimensionless parameter, p/d, being "p" the depth of the slot formed by the plates and "d" the distance between two plates. Were investigated sections from p/d = 1.66 up to p/d = 10.0. As regarding mean turbulent quantities, all features stressed in the previous papers were confirmed. When attention was pointed to large scale structures, the authors observed flow pulsations for $p/d \geq 2$, confirming results by using flow visualizations. A correlation for the Strouhal number was also proposed. The Strouhal number were based on the main frequency, the square root of the product of "p" and "d and the edge velocity, measured at edge of plates, U_{ed}. Therefore, the results showed discrepancies for p/d values greater than 7.

One of the tree compound channels studied by Meyer and Rehme (1995), was also investigated by Goulart and Möller (2006) and Goulart and Möller (2007). In the first work (Goulart and Möller, 2006), the authors investigated a rectangular channel with two parallel plates attached on the lateral wall. By using hot wires were performed measurements of two components of velocities for six test sections. For test sections depth-width ratio remained constant p/d = 5, even though dimensional parameters, "p, "d", could be different.

Despite the findings reported by Meyer and Rehme (1995), large-scale structures could not be found in all test sections, but only in that one with the smallest width, "d".

The conclusions led to a second investigation that showed the strong relationship between axial velocities profiles and the presence of large-scales structures. In Goulart and Möller (2007), the authors were succeeded in obtaining comprehensive measurements of the axial and transversal velocities fluctuations in ten test sections, involving three p/d ratios, 5, 10 and 12.50. The results showed a steady state plane turbulent mixing layer in spatial development between the plates. By using self-similarity functions it was possible to describe mean axial velocity (at the symmetry lines) as a tangent hyperbolic function. Related to flow large-scales appearances, an attempt to make a correlation for Strouhal number was done. The Strouhal number was defined as that one showed in mixing layer problems, using mixing layer thickness, $\delta_{(x)}$, as length scale, and the convection velocity, U_c, as velocity scale. The Strouhal numbers remained constant even for the deepest test section, where p/d = 12.50.

Again, attention is focused on overall features of the developing mixing layer in two sorts of compound channels. The first one concerns to a rectangular main channel connected to a narrow gap. In the second part, the main channel was splitted and two main channels connected by a gap are formed. This work is also an attempt to develop a methodology for handling problems involving rod bundles assemblies.

2. TEST SECTION AND EXPERIEMTNAL TECHNIQUE

The test section, Figure 2, consists in a 3320 mm long channel where both width, "W", and height, "H", are variable. While dimension "H", is increased in the range of 54 to 60 (mm), three different values, for "W", were adopted, namely 75, 120 and 130 mm. A splitter plate was placed along of its longitudinal dimension to reduce the height of the wind channel, Figure 2 (a). Working fluid was air at room temperature, driven by a centrifugal blower controlled by a frequency inverter, reaching the test section with about 1% turbulence intensity. A Pitot tube, placed on a fixed position upstream of the test section, was used to measure the reference velocity U_{ref} of the experiments. During the experiments the reference velocity, U_{ref}, remained almost constant.

Inside the channel two different topologies of compound channels were built. In the first one, two rectangular aluminium bars with thickness e = 1.2 mm and length "L" were attached on a side wall of the wind channel, Figure 2 (b). Main dimensions are the depth "p" and width "d". Another topology consists in moving these bars towards the

center of the channel forming two subchannels connected by a central gap with same width and depth, “d” and “p”, respectively, Figure 2(d). Coordinates system is placed as shown in Figure 2 (e) and (f).

The first topology will be called, thereafter, “SS” and the second one “DS”. These names are suitable, in the first case there is only one main subchannel (single-subchannel), and in the second case, there are two main subchannels (double-subchannel).

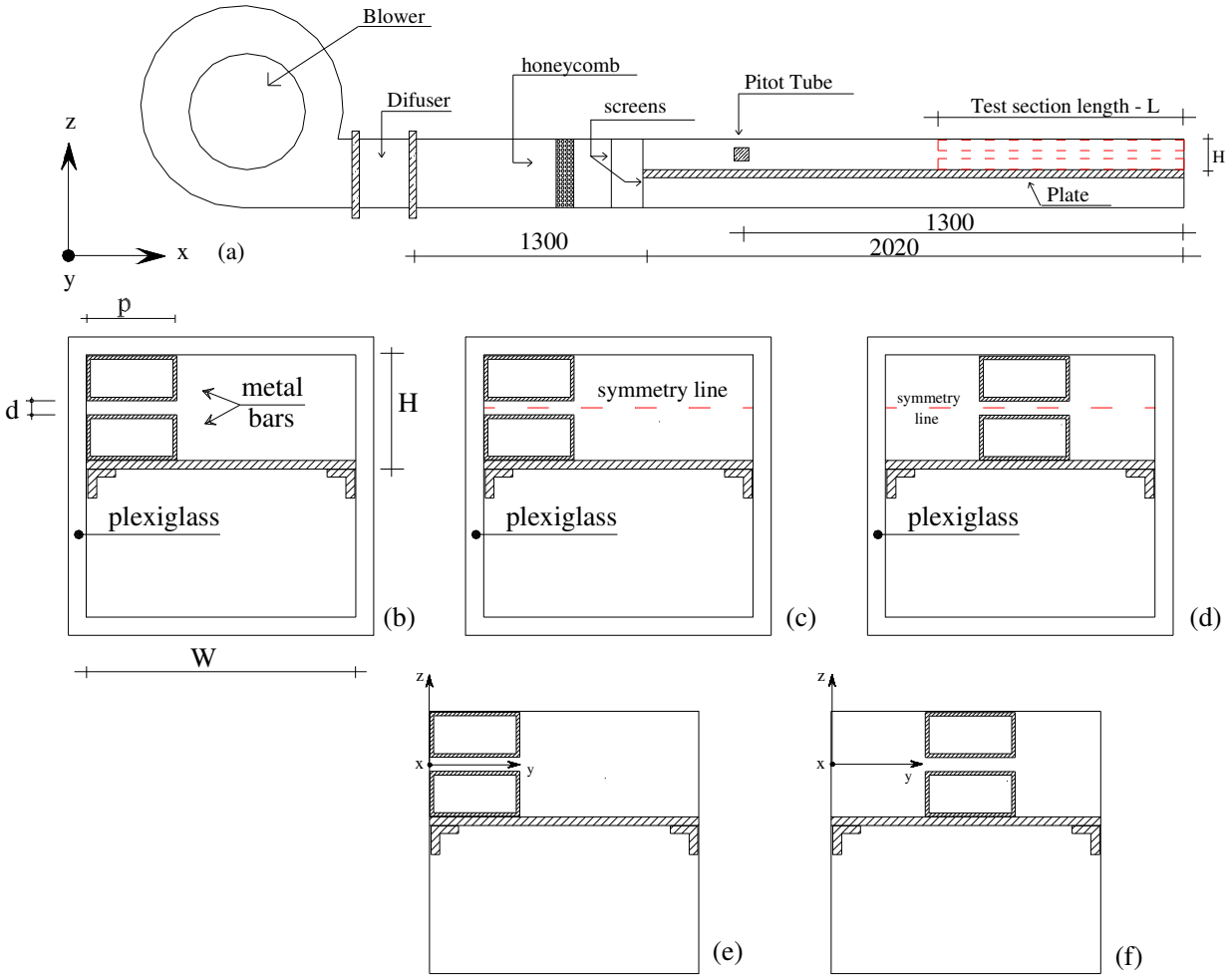

Figure 2 – Schematic view of the test section. Cross-section and coordinate system for each test section configuration.

Four different configurations were investigated for each topology, Table 1. By working with the same concepts used in the previous paper, Goulart and Möller (2007), Reynolds numbers were defined using as velocity scale the difference between upper and lower velocities from the mixing layer and as length scale, the mixing layer thickness, $\delta_{(x)}$. This definition is very usual in problems involving open compound channels, and, seemingly, provides a better comprehension of the flow. Using the criteria adopted, the experiments were performed within Reynolds number from 5.12 x 10³ up to 16.00 x 10³.

Table 1 – Test section configurations and Reynolds number – (Dimensions in mm).

Test section #	w	p	d	L	p/d	w/p	U_{ref} m/s	$Re = \frac{\Delta U \times \delta_{(x)}}{\nu}$
SS-01	130	50	10	1250	5.00	2.60	13.20	14.20×10^3
SS-02	130	50	4	1250	12.50	2.60	13.25	16.00×10^3
SS-03	120	38	4	1000	9.50	3.15	13.15	8.00×10^3
SS-04	75	25	4	500	6.25	3.00	13.22	8.05×10^3
DS-05	130	50	10	1250	5.00	2.60	13.20	11.99×10^3
DS-06	130	50	4	1250	12.50	2.60	13.26	12.76×10^3
DS-07	120	38	4	1000	9.50	3.15	13.14	11.49×10^3
DS-08	75	25	4	500	6.25	3.00	13.15	5.12×10^3

Measurements of velocity and velocity fluctuations were performed by a hot wire DANTEC StreamLine system using a double wire probe. This probe has a slant wire (45°) and a wire perpendicular to the main flow to perform simultaneous measurements of the transversal (y – parallel to the symmetry line, Figure 2(c) and (d)) and axial components (u) of the velocity vector. All measurements were performed 20 mm upstream of the channel outlet.

Collis and Williams (1959), method with modifications by Olinto and Möller (2004), was applied for the evaluation of the anemometer signals. Velocity field was previously measured by a Pitot tube.

Data acquisition was performed by means of a 16 bit National Instruments NI USB – 9162 A/D converter board, with a sampling frequency of 3 KHz and a low pass filter set at 1 KHz. Temporal series were 43.69 s long.

3. RESULTS AND DISCUSSION

3.1. Velocity Profiles

Figure 3 (a), shows mean axial velocity distribution and its derivative form, both are presented in a dimensionless form, by using its maximum values. A field of axial velocity is stressed in Figure 3 (b), at this time results are presented in non-dimensionless form. Both pictures are in good agreement with those presented in Meyer and Rehme (1994). Different authors have reported similar behavior that one found here. One can see flow acceleration towards the main channel followed by a velocity reduction in the narrow gaps, and peaks of vorticity at the interface main channel/sot, as well. Previous research has been treated this kind of flow as a bounded spatial developing mixing layer beginning at the narrow gap region and extending towards the main channel (Goulart and Möller, 2007).

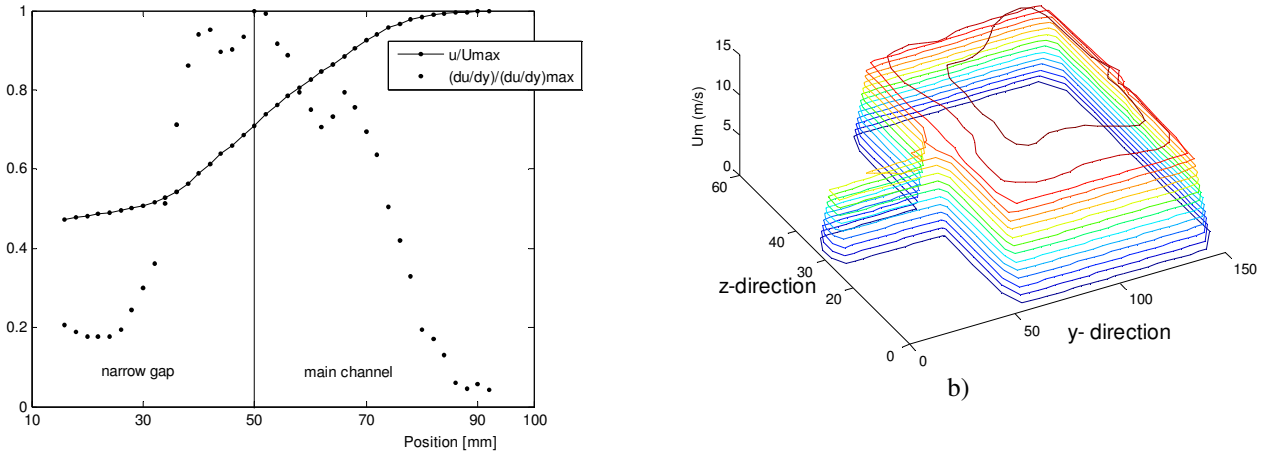

Figure 3 – Axial velocity distribution – SS-01. (a) mean axial velocity profile. (b) 3-D – plot of mean axial velocity field.

Mixing layer are characterized by the presence of two mains streams with different velocities, the highest one, U_2, and the lowest, U_1. Between them, the velocity profile can be established as a function of the self-similarity proprieties. In bounded mixing layers, generated by a narrow gap, the wall influence is important for U_1 evaluation, being necessary to determine the position where wall influence ends and the beginning of the shear layer. This is the location of the lower velocity U_1. Related to the upper velocity, U_2, this one takes place at the main channel, and represents the highest value of the mean axial velocity in the profile. Figure 4 presents how mean axial velocity profile was divided: at the zone 1, the velocity profile suffers from wall influence, while zone 2 represents the mixing layer itself.

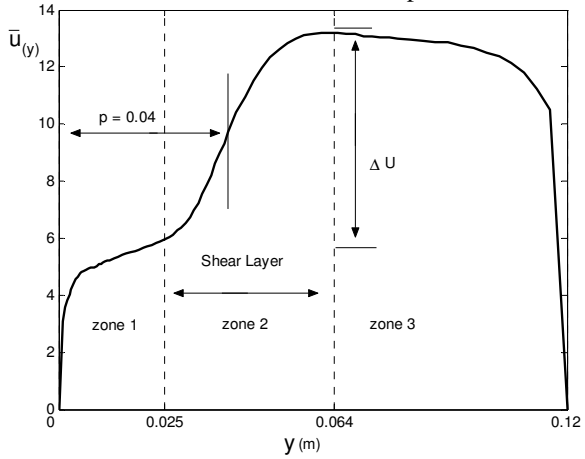

Figure 4 – Axial velocity profile on symmetry line of a compound channel. Goulart and Möller (2007).

The lower velocity, U_1, is defined as the velocity value where the velocity gradient changes its concavity, then, at this position,

$$\left.\frac{\partial^2 \bar{u}}{\partial y^2}\right|_{y_1} = 0 \tag{1}$$

By following this short explanation, it is expected that two main channels connected by the same narrow gap give rise two mixing layers, on the both sides of the narrow gaps. These mixing layer are formed due to viscous effects inside de slot. When the flow reaches the slot viscous forces act decreasing the velocity of the flow in the slot and increasing the velocity flow in the main channel. By this way two main streams with different velocities are formed giving rise mixing layer.

Mean axial velocity profile and its gradient, from test section DS-08, are presented in Figure 5 (a) and (b). Both are measured on the symmetry line being depicted as a y-axis function.

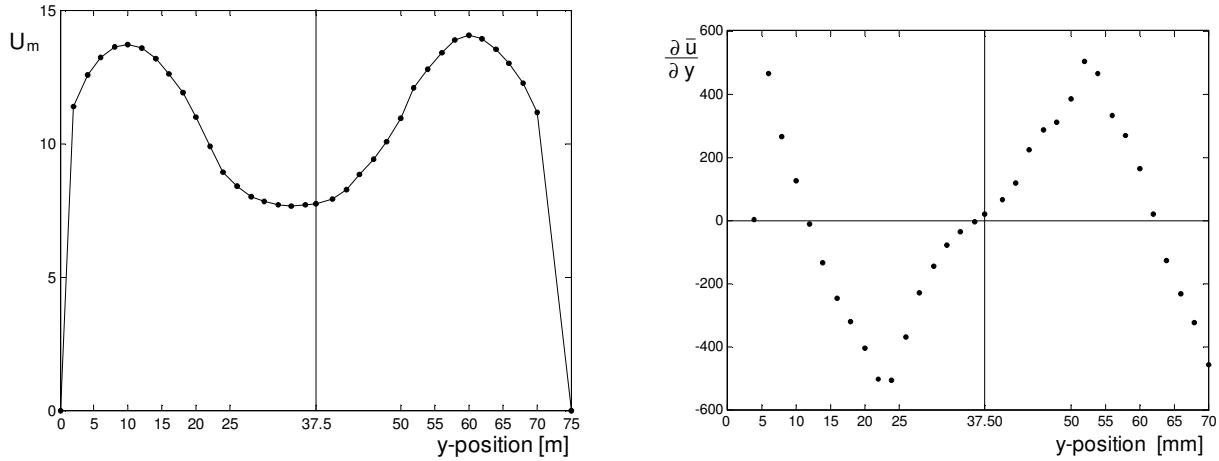

a) b)

Figure 5 – Mean axial velocity profiles on each side of the narrow gap. (b) mean velocity gradient.

The solid line in Figure 5 (a) shows the central gap reference. As predicted, two mixing layers are formed in both sides of the channel. Therefore, a small difference between both sides can be observed, showing entrance effects are still present. Another remarkable feature concerns to the position where U_1 takes place. In this kind of configuration, the upper velocity of the mixing layer, U_2, occurs in the main channels (both sides). Related to lower velocity, U_1, is expected find it at central position of the gap, however, this configuration will just be achieved when the entrance length is long enough.

Figure 5 (b) shows the derivative of the axial velocity profile ($\partial u/\partial y$). At the centers of mixing layers derivative shows its highest value (almost the same values on both sides), on the other hand, at the center of the gap its value is null, showing U_1, location.

Although, all test section studied show the same characteristic, the symmetry of the velocity profiles was not achieved for all test sections in the "DS" configuration. However, it is important to note main features discussed before, on velocities distribution, are showed in all tests sections.

3.2. Velocity distribution in mixing layers

As observed, it is possible to describe this problem as a steady state plane turbulent mixing layer in spatial development, and its two dimensional form can be written as follow,

$$\bar{u}\frac{\partial \bar{u}}{\partial x} + \bar{v}\frac{\partial \bar{u}}{\partial y} + \frac{\partial \overline{u'v'}}{\partial y} = \nu\frac{\partial^2 \bar{u}}{\partial y^2} \tag{2}$$

where $\bar{u}$, $\bar{v}$, are axial and transversal velocity components respectively and ν is the molecular (kinematic) viscosity. Being, $\overline{u'v'}$, shear stresses caused by velocity fluctuation.

According to Lesieur (1997), the self-similar solution for the Eq. (2), leads to an error function for the mixing layer velocity profile, however, a hyperbolic tangent function (tanh) is widely used as an approximation, thus

$$\bar{u}(\eta) = U_c + \frac{\Delta U}{2}\tanh(\eta) \tag{3}$$

where:

ΔU = difference between the lower and the upper velocities in the mixing layer, U_1 and U_2, respectively;

U_c = convection velocity, defined by

$$U_c = \frac{U_2 + U_1}{2} \tag{4}$$

η = similarity parameter, is given by Eq. (5)

$$\eta = 2\frac{y - y_c}{\delta_{(x)}} \tag{5}$$

where
y_c = coordinate of the center of the mixing layer;
$\delta_{(x)}$ = mixing layer thickness, Eq. (6)

$$\delta_{(x)} = \frac{U_2 - U_1}{\left.\frac{\partial \bar{u}}{\partial y}\right|_{max.}} \tag{6}$$

Figure 6 (a) (b) and (c), shows the velocity profiles of test sections types SS ad DS (last one left and right sides, respectively). Experimental data were plotted as a function of the similarity parameter, η, and fitted by using Eq. (7)

$$U_{ad} = 2\frac{\bar{u}(\eta) - U_c}{\Delta U} = \tanh(\eta) \tag{7}$$

Indeed, the hyperbolic tangent function presented a good agreement with experimental data, for all cases investigated. Therefore, some discrepancies were found, mainly at the edges of the profiles. An attempt to fit better velocities profiles an error functions was also used. However, no important improvements were done.

When one takes a look, more carefully, Figure 6 (b) and (c), is remarkable the asymmetry of the flow in the different main channels, see test sections DS 06 and 07. In these sections the main channel of right side seems to be more developed than left side.

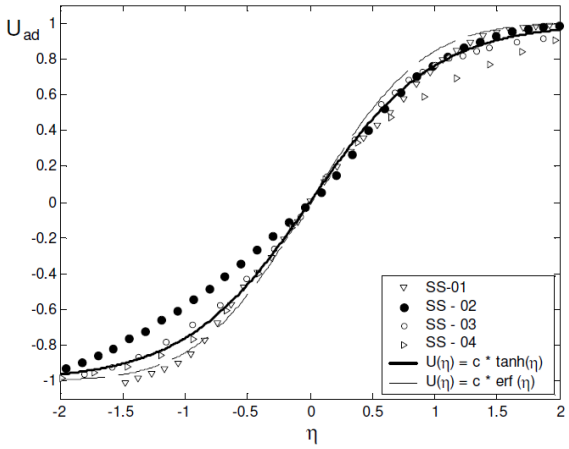

a)

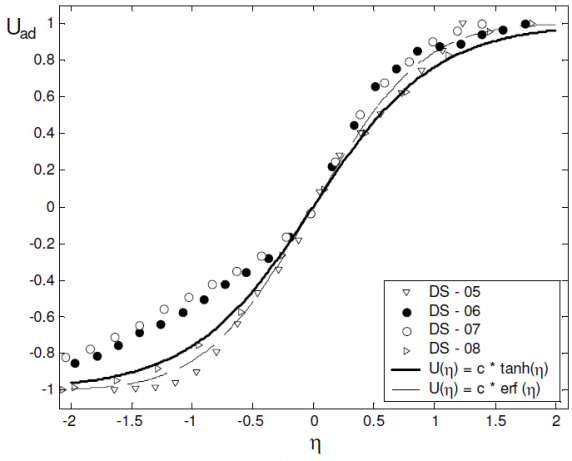

b)

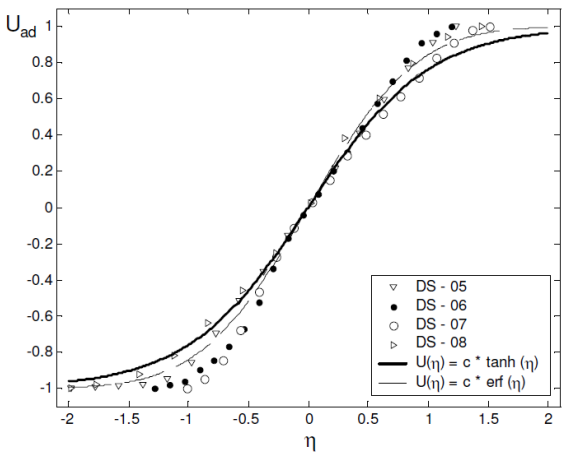

c)

Figure 6 – Mean axial velocity distribution in the mixing layer and its approximation by hyperbolic tangent function. a) section type SS. b) section type DS – left side. c) section type DS – right side.

Since self-similarity is attained, flow quantities are only dependent on local variables, including mean velocities, its fluctuations. In this state the increasing of mixing layer thickness, δ, is expected to be a linear functions of streamwise position.

Figure 7, shows the width of shear layer as a function of section test length "X", for both configurations. Width of the shear layer was obtained by using Eq. (6). Despite the scattering of the data, a linear fit seems to be adequate for the data from first configuration, SS, curve "A". However, DS configuration, cannot be fitted by linear approach. Non-linear dependence between mixing layer thickness and streamwise distance may suggest that the self-similar state has not been attained for all test sections in this configuration.

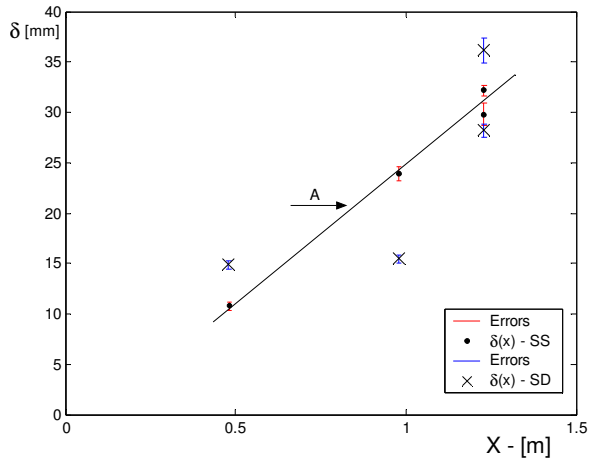

Figure 7 – Mixing layer growth as downstream distance function.

3.3. Reynolds stresses distribution and autospectral results

The profiles for the Reynolds normal stresses ($\overline{u'^2}$, $\overline{v'^2}$) and the shear stress, $\overline{u'v'}$, are presented in Figure 8 and Figure 9. Values are stressed in dimensionless form by using the velocity difference (U_2 - U_1) and plotted as a function of self-similarity coordinate.

For all cases Reynolds normal stresses and shear stress showed same features had already been found in previous works. Oster Wygnanski (1982) and Bell and Metha (1990), performed measurements in a developing mixing layer generated by a split plate. Results were quite similar to those found here, maximum value appeared at the central point of mixing layer, η = 0, decreasing towards main channel.

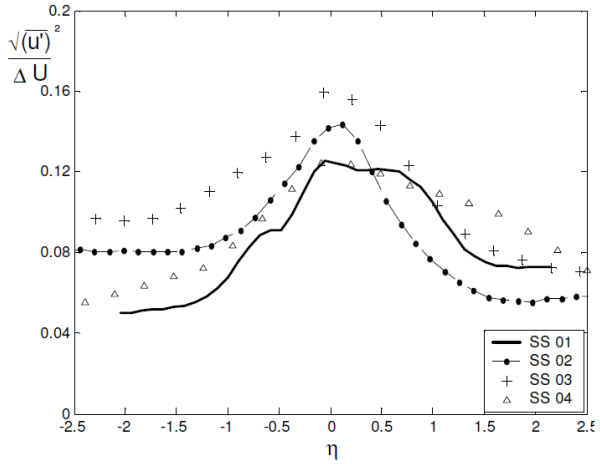

a)

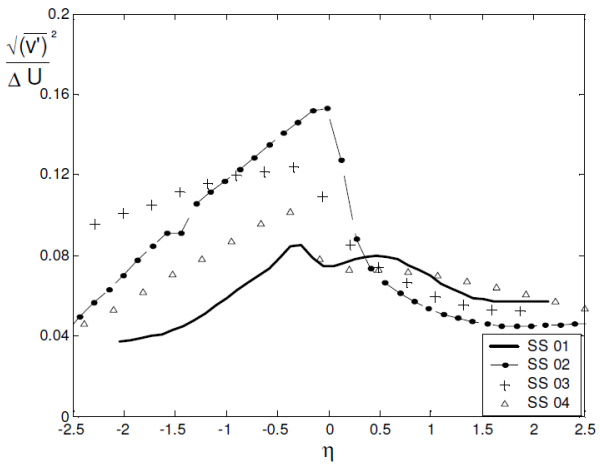

b)

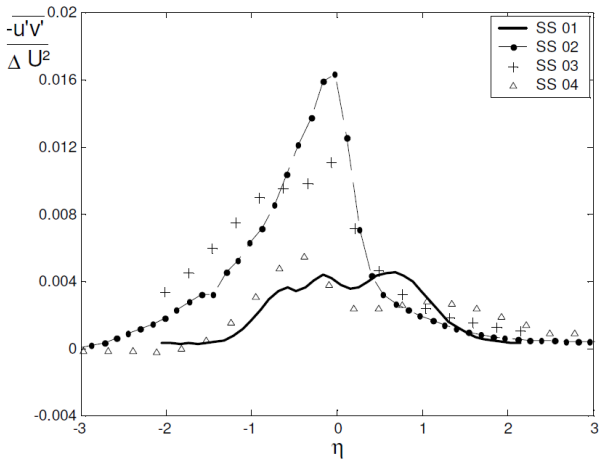

c)

Figure 8 – Profiles of normal Reynolds stresses and shear stress, test section type SS.

Figure 9 (a), (b) and Figure 10 (a) and (b), show normal Reynolds stresses and shear stress quantities in the second configuration, DS.

As expected, peaks of normal Reynolds stresses and shear stress appear on the both sides of narrow gap, at $\eta = 0$. These ones are produced by two developing mixing layers, as mentioned before. A lack of symmetry was almost typical characteristic for "DS" configurations, with exception section test DS – 08. Values of normal Reynolds stresses and shear stress measured in the right side main channel are higher than those found in the left side. It may suggest the flow developing is still not complete.

However, important features of mixing layer are present in the results, Figure 8 (c) and Figure 10 (b). These ones show shear stresses distribution for SS and DS test sections. There one can see null values for shear stresses out side mixing layer, as discussed in Townsend, 1976.

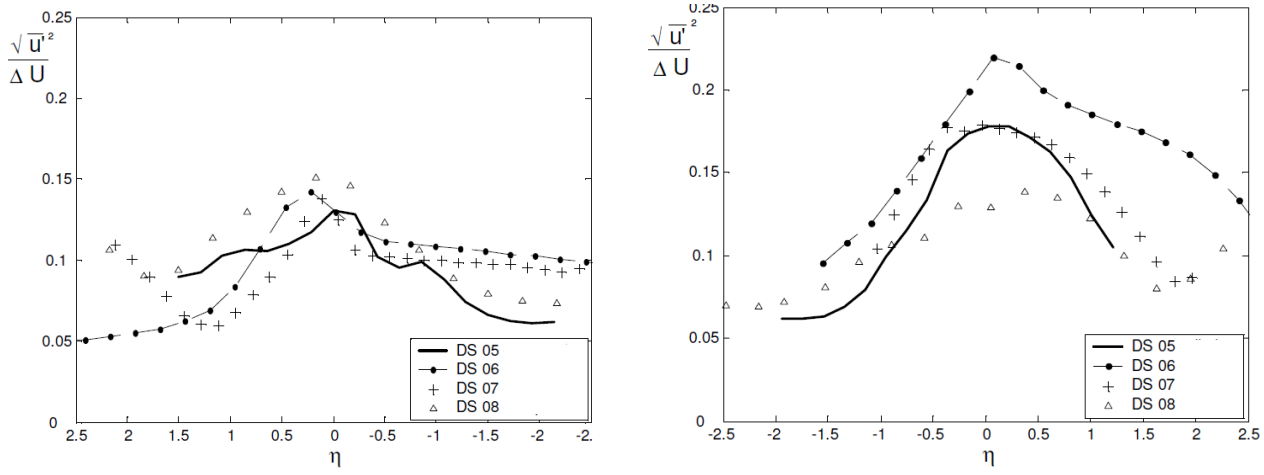

a) b)

Figure 9 - Profiles of normal Reynolds stresses and shear stress for DS topology. a) Normal Reynolds stress, $\sqrt{u'^2}/\Delta U$, for left side. b) Normal Reynolds stress, $\sqrt{u'^2}/\Delta U$, for left side right side.

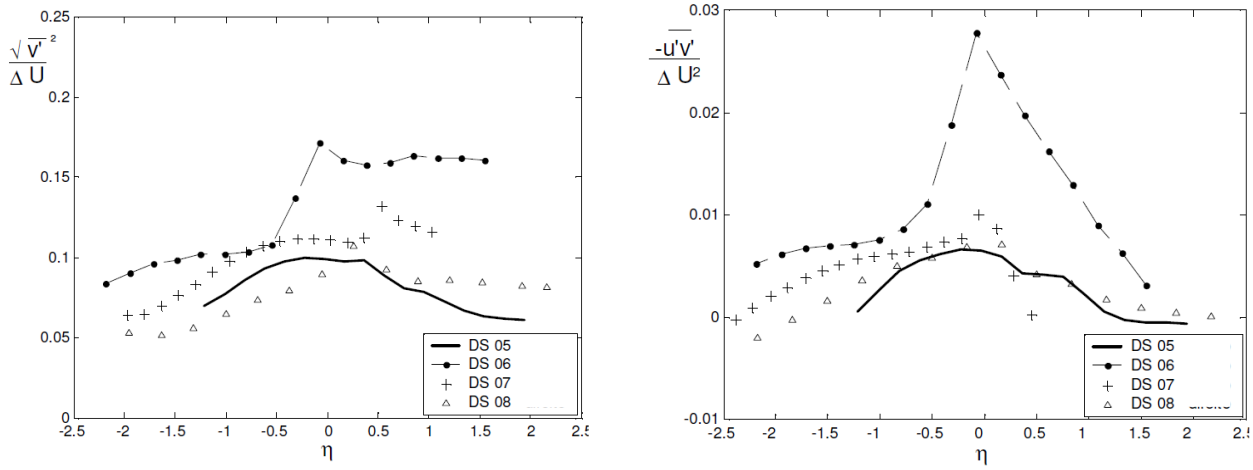

a) b)

Figure 10 – Normal Reynolds stress and shear stress, for DS configuration. a) Normal Reynolds stress, $\sqrt{v'^2}/\Delta U$, for right side. b) Shear stress, $-\overline{u'v'}/\Delta U^2$, for right side

Investigations on coherent structures in the flow were also performed for both velocity components, in all test sections Figure 11 (a) and (b).

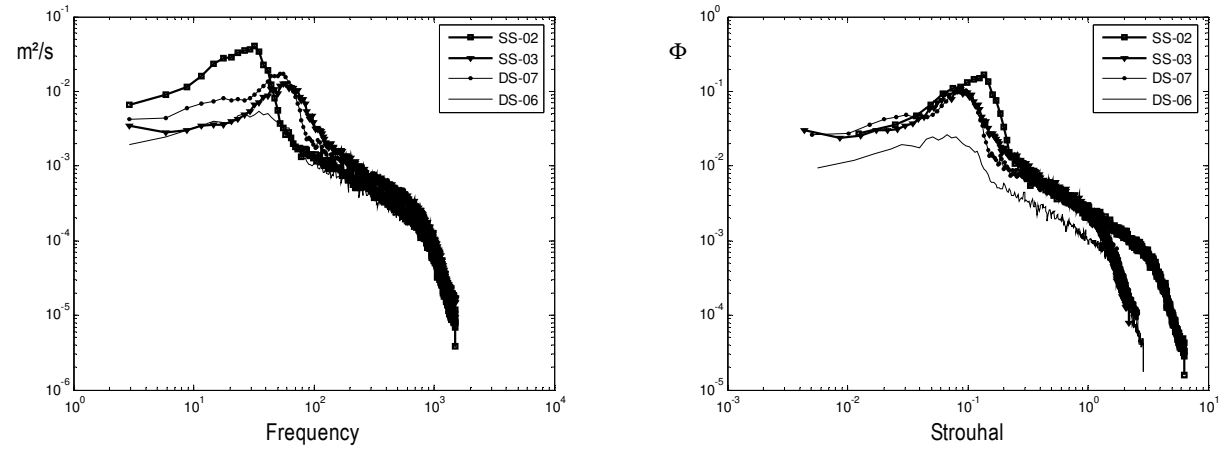

a) b)

Figure 11 – Autospectral densities. Test sections SS and DS.

Figure 11, shows autospectral density functions, velocities series was taken at η = -0.33. Uncertainties about autospectral results were form 2% up to 9%.

Energy (y-axis) and frequencies (x-axis), were made dimensionless by using own mean flow scales. The Strouhal number was formed with convective velocity, Uc, main frequency, f, and mixing layer thickness, $\delta_{(x)}$, Eq. (8), while, Φ , is given by Eq. (9).

$$St = \frac{f\,\delta_{(x)}}{U_c} \tag{8}$$

$$\Phi = \frac{\overline{u'^2}}{\delta_{(x)}\Delta U Hz} \tag{9}$$

This Strouhal number configuration is very usual in problems involving mixing layer generated by a split plate. Different authors have presented their reports showing this configuration is very suitable for these problems, with Strouhal number ranged 0.15, Bonnet at al., 1998.

Although same Strouhal number was not attained, mixing layer thickness, $\delta_{(x)}$, and convection velocity, U_c, seems to be very suitable for problems involving compound channels. Note, when frequencies are put on dimensionless form, Figure 11 (b), peaks stay closer than Figure 11 (a).

Furthermore, it is important to see spectral density function for two different compound channels, SS and DS topology, can be plotted together. This fact indicates purposed Strouhal number is general enough for this kind of problem.

4. CONCLIDING REMARKS

In this paper, an experimental study of mean and fluctuating velocities of the turbulent flow in two sorts of compound channels was performed. The main purpose was the investigation of the flow characteristics in these two different channels and an attempt to describe mean quantities as self-similarity functions, such as done in a previous paper, Goulart and Möller (2007).

The results of the velocity measurements showed the presence of a shear layer in both configurations investigated. The mean and fluctuating quantities distribution reminded as self similarity function, showing the self preserving characteristics of the flow. Therefore, for DS configuration test sections, entrance effects were still present, being this fact pointed by asymmetrical behavior of mean quantities profile, on the symmetry line.

Spectral investigations, by means of Strouhal number, defined with the main frequency component of the velocity fluctuation, the convection velocity and the shear layer thickness, were performed. Although, the Strouhal number, as defined, have led to good results, lower values than those generated by two plates, St = 0.17, were obtained. However, purposed Strouhal number seem to be suitable for closed compound channels problems, once it is general enough to describe frequencies from two different kinds of compound channels.

5. ACKNOWLEDGEMENTS

The support by the CNPq – Brazilian Scientifical and Technological Council is grateful acknowledged.
Jhon N. V. Goulart thanks also the CNPq for granting him a fellowship.

6. REFERÊNCIAS

Bell, J.H., Mehta, R. D. 1990, Two-Stream Mixing Layer from Boundary Layers, AIAA Journal, v. 28, pp: 2034-2042.

Collis, D. C. and Willans, M. J., Two-dimensional convection from heated wires at low Reynolds numbers, J. Fluid Mech., 6, 357-384, 1959.

Goulart, J. N. V. and Möller, S. V., Flow pulsations in short compound channels. In: 11º Congresso Brasileiro de Engenharia e Ciências Térmicas - ENCIT, 2006, Coritiba, 2006.

Goulart, J. N. V. and Möller, S. V., Shear flow in compound channels. In: 19º International Congress of Mecahnical Engeneering - COBEM, 2007, Brasilia, 2007.

Knight, D.W. and Shiono, K., Turbulence measurements in a shear-layer region of a compound channel, Journal of Hydraulic Research, 28, 175-196, 1990.

Lesieur, M., Turbulence in Fluids. Third Edition, Kluwer Academic Publishers, Dordrecht, The Netherlands, 1997.

Meyer, L. and Rehme, K., Large-scale turbulence phenomena in compound rectangular channels, Experimental Thermal and Fluid Science, 8, 286-304, 1994.

Meyer, L. and Rehme, K., Periodic vortices in flow though channels with longitudinal slots or fins, 10th Symposium on Turbulent Shear Flows, The Pennsylvania State University, University Park, August 14-16, 1995.

Möller, S. V., On Phenomena of Turbulent Flow through Rod Bundles. Experimental Thermal and Fluid Science, 4, 25-35, 1991.

Olinto, C. R. and Möller, S. V., X-probe calibration using Collis and William's equation. In: 10º Congresso Brasileiro de Engenharia e Ciências Térmicas - ENCIT, 2004, Rio de Janeiro, 2004.

Oster, D. and Wygnanski, I. The forced mixing layer between parallel stream. J. Fluid Mech. 12, 91-130, 1982.

Prooijen, B. C. van and Uijttewaal, W. S. J., A linear approach for the evolution of coherent structures in shallow mixing layers, Physics of Fluids, 14, 4105-4114, 2002.

Rowe, D.S., Johnson, B.M. and Knudsen, J. G., Implications concerning rod bundle crossflow mixing based on measurements of turbulent flow structure, Int. J. Heat Mass Transfer, 17, 407-419, 1974.

Soldini, L., Piattella, A., Brocchini, M., Mancinelli, A. e Bernetti, R. Macrovortices-induced horizontal mixing in compound channels, Ocean Dynamics, 54, 333 – 339, 2004.

Townsend, A. A., The structure of turbulent shear flow. Cambridge University Press, Cambridge, England, 1976, 188-230.

Wu, X. and Trupp, A. C., Spectral measurements and mixing correlations in a simulated rod bundle subchannels, Int. J. Heat Transfer, 37, 1277-1281, 1994.

7. RESPONSIBILITY NOTICE

The authors are the only responsible for the printed material included in this paper.